

**Are your MRI contrast agents cost-effective?**

Learn more about generic Gadolinium-Based Contrast Agents.



**FRESENIUS  
KABI**

caring for life

**AJNR**

**Diffusion Tensor Imaging Screening of  
Radiation-Induced Changes in the White  
Matter after Prophylactic Cranial Irradiation  
of Patients with Small Cell Lung Cancer:  
First Results of a Prospective Study**

This information is current as  
of April 23, 2024.

T. Welzel, A. Niethammer, U. Mende, S. Heiland, F. Wenz,  
J. Debus and R. Krempien

*AJNR Am J Neuroradiol* 2008, 29 (2) 379-383

doi: <https://doi.org/10.3174/ajnr.A0797>

<http://www.ajnr.org/content/29/2/379>

## ORIGINAL RESEARCH

T. Welzel  
A. Niethammer  
U. Mende  
S. Heiland  
F. Wenz  
J. Debus  
R. Krempien

# Diffusion Tensor Imaging Screening of Radiation-Induced Changes in the White Matter after Prophylactic Cranial Irradiation of Patients with Small Cell Lung Cancer: First Results of a Prospective Study

**BACKGROUND AND PURPOSE:** Diffusion tensor imaging (DTI) will show abnormal fractional anisotropy (FA) in the normal-appearing brain after prophylactic cranial irradiation (PCI). These abnormalities will be more accentuated in patients with underlying vascular risk factors.

**MATERIALS AND METHODS:** A prospective study by use of DTI and conventional T2-weighted MR images was performed with a 1.5T unit with 16 patients with small cell lung cancer and undergoing PCI. All of the T2-weighted images were evaluated with respect to abnormalities in signal intensity of white matter as markers of radiation damage. Measurements of FA were performed before, at the end of, and 6 weeks after radiation therapy. On the FA maps, the bifrontal white matter, the corona radiata, the cerebellum, and the brain stem were evaluated. FA values were compared with respect to age, demographic, and vascular risk factors. Statistical analyses (Friedman test, Wilcoxon test, and Mann-Whitney *U* test) were performed.

**RESULTS:** Fractional anisotropy decreased significantly in supratentorial and infratentorial normal-appearing white matter from the beginning to the end of PCI ( $P < .01$ ). A further decline in FA occurred 6 weeks after irradiation ( $P < .05$ ). A stronger reduction in FA was observed in patients with more than 1 vascular risk factor. There was an age-related reduction of white matter FA. Patients 65 years and older showed a trend toward a stronger reduction in FA.

**CONCLUSION:** During the acute phase, after PCI, patients with many vascular risk factors showed stronger damage in the white matter compared with patients with only 1 risk factor.

White matter (WM) is recognized as the element in the brain that is most vulnerable to irradiation.<sup>1,2</sup> Postmortem studies show a broad spectrum of radiation changes ranging from vascular damage to coagulation necrosis.<sup>1</sup> Sheline differentiates among 3 phases of the pathophysiological reaction to irradiation in the normal brain tissue.<sup>3</sup> In the acute phase, after the first few fractions of irradiation, only focal damage dominates. An additional occurrence of glial glycogen depositions is generally completely reversible, and necrosis caused by irradiation is a rare exception. Subacute changes after irradiation occur weeks to months after the irradiation, predominantly due to cell death of myelin-producing oligodendrocytes. After a temporary demyelination, a growth of oligodendrocytes and remyelination of the brain tissue follow.<sup>3,4</sup> The chronic phase of the radiation changes is marked by diffuse changes due to wall thickening of the vascular structures, decreasing the number of glial-supporting cells, and diffuse demyelination.<sup>5</sup> The white substance of the brain is significantly more affected in the diffuse damage of brain tissue because of the failure of the glial support system. Neuroradio-

logic studies show chronic diffuse changes ranging from 38% to 100% of patients.<sup>1</sup>

The first MR imaging studies to detect radiation changes were carried out in the 1980s. MR imaging has proven to be a very sensitive instrument to detect axonal demyelination and vasogenic brain edema caused by capillary endothelial damage, because these lesions result in a prolongation of the T2 relaxation time.

On conventional MR images, posttreatment changes of the WM often begin as hyperintense foci in the deep WM. The changes in the WM are adjacent to the anterior and posterior horns of the lateral ventricles, progressing to more peripheral regions in the centrum semiovale, and then coalescing to involve the entire WM. The WM of the brain stem, the cerebellum, the internal capsules, and the basal ganglia are relatively spared.<sup>5-8</sup>

Most studies have shown that conventional MR imaging is of limited benefit, because the sequences are not sensitive enough to depict early injury after irradiation.<sup>6,7</sup> However, new MR imaging sequences, like diffusion tensor imaging (DTI), allow an in vivo examination of the microstructure of the brain tissue.<sup>8</sup> Khong et al<sup>9,10</sup> studied the long-term effects of high-dose cranial irradiation and chemotherapy on the brain in medulloblastoma patients. When performing DTI fractional anisotropy (FA), earlier studies show a decrease in many regions of the WM of medulloblastoma patients compared with that of healthy subjects.<sup>9-11</sup> The authors hypothesize that, in treatment-induced WM injury, loss of anisotropy would occur as a result of ischemia, demyelination, and gliosis.

Received April 27, 2007; accepted after revision July 18.

From the Departments of Radiooncology (T.W., A.N., U.M., J.D., R.K.) and Neuroradiology (S.H.), University of Heidelberg, Heidelberg, Germany; and Department of Radiooncology (F.W.), University of Heidelberg, Mannheim, Germany.

This work was financed by a grant (KR 1942/1-1) from the Deutsche Forschungsgemeinschaft.

Please address correspondence to Thomas Welzel, Department of Radiooncology, University of Heidelberg, Im Neuenheimer Feld 400, 69120 Heidelberg, Germany; e-mail: thomas.welzel@med.uni-heidelberg.de

DOI 10.3174/ajnr.A0797

Recent population-based studies have demonstrated a correlation between WM lesions (WML; also known as leukoaraiosis) and vascular risk factors.<sup>12,13</sup> Because of that, we documented the clinical risk factors for cerebral vessel disease, like diabetes, hypertonus, alcohol, and smoking. We hypothesize that there is a synergistic effect of radiation-induced and vascular-induced damage of the WM in patients without preexisting brain abnormalities shortly after PCI.

## Materials and Methods

### Patients

Sixteen patients with small-cell lung cancer who had been diagnosed recently were enrolled. The age of the 6 female and 10 male patients ranged from 45 to 67 years (median, 57 years). Prophylactic cranial irradiation (PCI) is offered as a routine examination to patients with limited small cell lung cancer. This form of radiation therapy (RT) reduces the incidence of brain metastases significantly and improves the overall survival.<sup>14</sup> The RT (total dose, 30 Gy) in 2-Gy daily fractions was given after chemotherapy. The target volume was treated with opposed lateral isocentric fields with photons from a 6-MeV linear accelerator (Siemens, Concord, Calif). The chemotherapy regimen was carboplatin/etoposid (CPE protocol), cisplatin/etoposid (PE protocol), or doxorubicin/cyclophosphamid/vincristin (ACO protocol). At the time of imaging, none of the patients had begun steroid or phenytoin treatment. No patient had received cranial irradiation or cranial surgery before beginning PCI. Measurements of FA were performed before, at the end of, and at 6 weeks after RT. At the beginning of irradiation, all of the patients had normal MR imaging (with gadolinium) of the brain and no history of brain tumors or metastases and neurologic deficits. Each patient signed a declaration of information and consent. The final protocol was approved by the ethics committee. The study complied with the Helsinki Declaration, the American Medical Association's professional code of conduct, the principles of Good Clinical Practice guidelines, and the Federal Data Protection Act. The trial was also carried out according to local legal and regulatory requirements.

### MR Imaging

All of the MR images were obtained with a 1.5T unit (Symphony; Siemens, Erlangen, Germany) by using a standard head coil. The following sequences were performed in all of the patients: axial T2-weighted imaging (TR/TE, 4000/100 ms; section thickness, 5 mm with 1.5-mm gap; and FOV, 230 mm). Conventional fast spin-echo T2-weighted MR images were evaluated for abnormalities of WM as markers of radiation damage.

DT imaging was performed by single-shot spin-echo-planar imaging (TR/TE, 7200/106 ms; FOV, 240 mm; acquisition matrix, 96 × 96 ms). By use of a section thickness of 3 mm, images were acquired through the entire brain (~44 images). Diffusion-sensitizing gradient encoding was applied in 6 directions using a high-diffusion weighting factor ( $b = 1000 \text{ s/mm}^2$ ), and 1 image was acquired without use of a diffusion gradient (ie,  $b = 0 \text{ s/mm}^2$ ). The gradient directions were chosen using the technique described by Bassler<sup>15</sup> and Bassler and Jones.<sup>16</sup>

A total of 308 images were obtained of the brain volume. The measurements were repeated 8 times, yielding an approximate total of 2464 images. DTI time was approximately 7 minutes and 44 seconds (1 sequence, 58 seconds). The section locations were identical for all of the follow-up examinations. The diffusion-weighted MR images

were transferred to an Advantage Workstation (GE Healthcare, UK) for data processing. Maps of FA were generated. The diffusion tensor and FA maps were calculated on a voxel-by-voxel basis with an in-house program implemented in Matlab (MathWorks, Natick, Mass).

### Region of Interest Analysis

All of the MR images were analyzed by 2 experienced radiologists (T.W. and R.K.) who worked independently; disagreements were resolved in consensus. The following anatomic sites were evaluated: 1) WM of the cerebellar hemispheres, 2) periventricular WM of the frontal lobes, 3) WM of the corona radiata, and 4) WM of the brain stem. The oval-shaped regions of interest (ROIs) were manually placed onto the FA maps. All of the ROIs were superimposed in an identical position onto the FA maps over all 3 of the measuring points. ROIs were widely placed in each hemisphere through normal-appearing WM. The regions next to the sulci were excluded to avoid partial volume effects of the gray matter and of the CSF.

### Statistical Analysis

Data were analyzed by using SPSS PC version 13.0.1 for Windows (SPSS, Cary, NC). Analyses included only data of patients who completed the study and did not have to be excluded. To assess changes in mean FA, data were submitted to Friedman test. When a statistical significance was reached, posthoc analyses were carried out with the Wilcoxon test. The level of significance was set at a 5% limit, with a Bonferroni correction for multiple comparisons. The mean FA values obtained in the left and right brain hemispheres were compared by using Mann-Whitney *U* tests. The influence of risk factors was controlled with Mann-Whitney *U* tests assessing rates of change (difference at the end of RT and 6 weeks later from baseline value in percentage). Wilcoxon (exact tests) were used to assess changes from the baseline. Differences were considered significant if the probability of error was  $P < .05$ .

## Results

FA levels in the cerebellum, frontal WM, and corona radiata were significantly lower during follow-up compared with baseline levels ( $P < .001$ ). There was no significant change in the brain stem (Table 1). Compared with the initial values, the FA decreased significantly after RT in the cerebellum, frontal WM, and corona radiata ( $P < .01$ ). Six weeks from the end of RT, a further decline in FA occurred in the frontal WM and corona radiata ( $P < .05$ ). The strongest decrease in FA levels was found in the WM of the cerebellar hemispheres, with a mean decline of  $-7.1\%$  and  $-7.9\%$  at the end and 6 weeks after the completion of RT, respectively, compared with the baseline ( $P < .05$ ). The FA in the corona radiata region declined by  $-3.9\%$  at the end and  $-5.7\%$  6 weeks after the completion of RT when compared with the baseline ( $P < .05$ ). The FA in the frontal WM region declined by  $-2.7\%$  at the end of RT and  $-5.2\%$  6 weeks after the completion of RT compared with the baseline ( $P < .05$ ).

Patients 65 years of age or older showed a trend toward a stronger reduction of FA compared with patients younger than 65 years of age in the cerebellum, frontal WM, and corona radiata. No differences were detected between men and women. A total of 38% of the patients had more than 1 risk factor, which included the following: hypertension 60%, smoking 88%, diabetes mellitus 60%, alcoholism 6%, and multiple regimen of chemotherapy treatment 6%. A more

**Table 1: Course of mean fractional anisotropy at different anatomic sites (*n* = 16)**

Variable	T0, Mean ± SD	T1, Mean ± SD	<i>P</i> *†	T2, Mean ± SD	<i>P</i> †	<i>P</i> ‡
CB	.173 ± .021	.161 ± .020	.000	.159 ± .016	.002	.000
FWM	.466 ± .063	.452 ± .056	.003	.442 ± .061	.000	.000
CR	.490 ± .035	.472 ± .044	.000	.463 ± .041	.000	.000
BS	.420 ± .048	.424 ± .043	.776	.434 ± .040	.121	.305

**Note:**—CB indicates bilateral cerebellar white matter; FWM, bilateral frontal white matter; CR, bilateral corona radiata; BS, brain stem; T0, at baseline; T1, at the end of radiotherapy; T2, at 6 weeks after radiotherapy.

\* *P* values are from Wilcoxon test (comparison between T0 and T1).

† *P* values are from Wilcoxon test (comparison between T0 and T2).

‡ *P* values are from Friedman test (comparison across time).

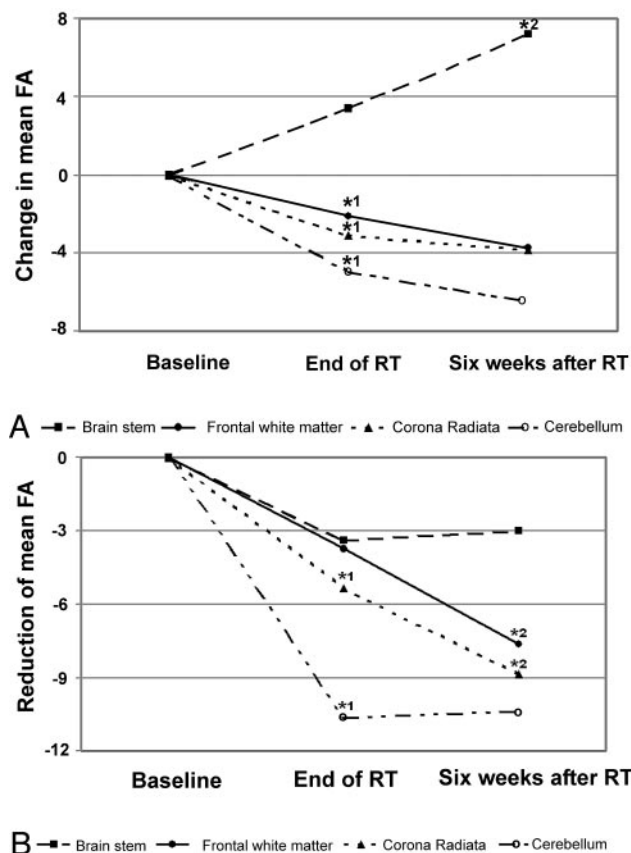


**Fig 1.** A, Change in mean fractional anisotropy in patients with 0 or 1 vascular risk factor (*n* = 10). \*1 indicates significant reduction from baseline (*P* < .05); \*2 indicates significant improvement from baseline (*P* < .05). B, Reduction of mean fractional anisotropy in patients with more than 1 vascular risk factor (*n* = 6). \*1 indicates significant reduction from baseline (*P* < .05); \*2 indicates further significant reduction from the end of RT (*P* < .05).

pronounced reduction of FA was seen on all of the anatomic sites in those patients with more than 1 risk factor (Fig 1A, -B). Patients with diabetes showed a trend toward a stronger decline in FA in all 4 of the brain regions at the end of RT when compared with patients without diabetes. Six weeks later there was a lower FA in the frontal region (*P* < .05) and corona radiata (*P* value not significant) in patients with diabetes. On the contrary, at 6 weeks after RT, the patients with 0 or 1 vascular risk factor showed a significant increase in FA of the brain stem as compared with the baseline (Fig 1A).

Differences between FA data of the right and left hemispheres are presented in Table 2. FA decreased most in the right (−8.7%) and left (−7.1%) cerebellum (*P* ≤ .001). The smallest reduction in FA was obtained in the frontal region (left frontal region: −5.6%; right frontal region: −4.8%; *P* <

.02). At the end of RT, there was a significant decrease in right-sided and left-sided FA levels (*P* < .01). Six weeks after RT, the FA decreased further in the right frontal lobe and right corona radiata (*P* < .01). Significant differences between right-sided and left-sided FA levels were not seen. There was no evidence of radiation-induced edema or demyelination spots on T2-weighted images after RT.

## Discussion

Several studies have recently reported the effectiveness of DTI for evaluation of WM lesions in predamaged brain tissue.<sup>9,17</sup> The findings of our study suggest that DTI can detect early WM changes of normal brain tissue induced by radiation. The pathogenesis of this damage is originated from vascular damage. A higher vascularity is reported in rodents at an early phase after high-dose whole-brain irradiation.<sup>18,19</sup> Damage of the WM in pig models induced by experimental radiation has shown an initial macrophage inflammation and vascular congestion followed by vascular endothelial and glial injury.<sup>20</sup>

Our results show that the FA values were lower in the WM in multiple anatomic sites after PCI. These prospective findings are consistent with previous retrospective studies that have shown that FA can be used as an index for evaluation of treatment-induced WM injury.<sup>9,17</sup> Khong et al<sup>9</sup> identified radiosensitive regions (frontal, corona radiata, cerebellum, and brain stem) in medulloblastoma patients after cranial irradiation. Our study confirms this radiosensitivity in normal brain tissue in the acute phase after RT. On the contrary, we found an increase in FA in the brain stem. This unexpected trend was also reported by Qiu et al.<sup>21</sup> They proposed 2 possible explanations: hemorrhagic effects or a selective damage of fiber tracts at regions of fiber crossing. Our study supports the idea of a selective damage of fiber tracts. The brain stem consists of multiple crossing points. A selective damage in this region may lead to more coherently oriented fiber tracts and, hence, increased FA despite the degeneration of fibers.<sup>21,22</sup>

Another MR method to estimate WM damage is diffusion-weighted imaging (DWI). DWI is a well-established method and has become important in imaging CNS abnormalities. It has been shown that DWI is able to detect WM lesions after radiation.<sup>23</sup> However, a recent study of patients with multiple sclerosis has demonstrated that the FA values are more sensitive in detecting lesions of normal-appearing WM in T2-weighted MR images than apparent diffusion coefficient values.<sup>24</sup>

DTI and proton MR spectroscopy allow quantitative investigation of changes in the metabolite level and water diffusion parameters of normal-appearing WM on conventional T2-weighted MR images.<sup>20,25</sup> In studies of proton magnetic reso-



**Table 2: Course of mean fractional anisotropy, left and right hemisphere (n = 16)**

Variable	T0, Mean $\pm$ SD	T1, Mean $\pm$ SD	$\Delta$ , %	P*	T2, Mean $\pm$ SD	$\Delta$ (%)	P†	P‡
CB								
Right	.173 $\pm$ .023	.162 $\pm$ .019	−6.1	.000	.160 $\pm$ .017	−7.1	.007	.001
Left	.174 $\pm$ .021	.160 $\pm$ .023	−8.0	.000	.158 $\pm$ .019	−8.7	.001	.000
FWM								
Right	.470 $\pm$ .069	.456 $\pm$ .058	−2.5	.008	.441 $\pm$ .056	−5.6	.007	.000
Left	.463 $\pm$ .060	.449 $\pm$ .058	−3.0	.003	.442 $\pm$ .070	−4.8	.015	.011
CR								
Right	.489 $\pm$ .031	.473 $\pm$ .040	−3.3	.001	.459 $\pm$ .036	−6.2	.000	.000
Left	.492 $\pm$ .043	.470 $\pm$ .053	−4.6	.001	.466 $\pm$ .049	−5.2	.000	.000

Note:—CB indicates cerebellar white matter; FWM, frontal white matter; CR, corona radiata; T0, at baseline; T1, at the end of radiotherapy; T2, at 6 weeks after radiotherapy.

\* P values are from Wilcoxon test (comparison between T0 and T1).

† P values are from Wilcoxon test (comparison between T0 and T2).

‡ P values are from Friedman test (comparison across time).

nance spectroscopy (MR spectroscopy) during and after radiation, a decrease of *N*-acetyl-L-aspartate was found 3 months after cranial irradiation (early delayed phase). In the acute phase there were no radiation-induced changes in the brain metabolism. Our study found radiation-induced changes in diffusion at the final stage of cranial irradiation (acute phase). We presume that DTI is a more sensitive method for in vivo estimation of neurotoxicity in the acute phase after irradiation than MR spectroscopy. Contrary to the study of Kitahara et al,<sup>17</sup> we followed a prospective study design with a strictly controlled follow-up MR imaging schedule. Kitahara et al<sup>17</sup> examined patients with different brain tumors and a predamaged tissue after surgery. Our study differs with regard to methodology. Furthermore, these authors evaluated only supraventricular regions.

The presented results confirm that vascular risk factors are related to WM (WML) after irradiation. Furthermore, we show that the combination of many vascular risk factors and radiation favor an early posttreatment onset of WML. We found that there is a stronger reduction of FA in patients older than 65 years of age after PCI. Some studies indicate poorer neurobehavioral outcome for elderly patients after cerebral irradiation.<sup>26,27</sup> Maire et al<sup>26</sup> showed a trend of declining intelligence quotient in adults older than 50 years of age in comparison with the 30- to 49-year-old group. Wassenberg et al<sup>27</sup> found more cognitive impairment related to RT in patients with lymphoma who were older than 60 years of age. Until now, the cerebral tissue has been seen as a late-reacting tissue; the presented results of this study and neurocognitive studies disprove this opinion.<sup>28</sup>

In our study, we demonstrate a better tolerance of brain parenchyma in patients with 0 or 1 vascular risk factor receiving irradiation (30 Gy total dose) compared with patients with more vascular risk factors. Consequently, brain parenchyma of those low-risk patients might tolerate an even higher irradiation dose; a better control of brain metastases could be accomplished.

The present study is limited because it was a feasibility study with a small number of patients. We were not able to correlate the radiation-induced WM injury with any change in clinical symptoms. Further study is warranted, especially to correlate clinical symptoms like neurocognitive deficits (eg, memory or attention) with radiation-induced reduction of anisotropy of WM. An additional trial is in preparation to involve a higher number of patients treated with different radiation techniques.

## Conclusions

In this prospective study, we successfully performed clinical DTI screening for detection of radiation-induced WM injury in the acute phase after RT. FA is a useful marker to describe in vivo changes in the microstructure of the brain tissue. A significant reduction in anisotropy is found in cerebellar, frontal WM, and corona radiata after PCI. An early detection of radiation-induced WM injury by DTI has the potential to alert the oncologist to this diagnosis and to provide a technique to monitor damage in the WM.

## Acknowledgments

We especially thank Thomas Wilhelm, PhD (Department of Neuroradiology), for his initial work developing the DTI sequences.

## References

- Valk PE, Dillon WP. Radiation injury of the brain. *AJNR Am J Neuroradiol* 1991;12:45–62
- Ball WS, Prenger EC, Ballard ET. Neurotoxicity of radio/chemotherapy in children: pathologic and MR correlation. *AJNR Am J Neuroradiol* 1992;13:761–76
- Sheline GE, Wara WM, Schmith V. Therapeutic irradiation and brain injury. *Int J Radiation Oncol Biol Phys* 1980;6:1215–28
- Lierse W. Experimentelle strahlenfolgen am hirngewebe. In: Heuck F, Scherer E, eds. *Handbuch der Medizinischen Radiologie*, Bd. 20, Berlin: Springer-Verlag; 1985:349–78
- Tsuruda JS, Kortman KE, Bradley WG, et al. Radiation effects on cerebral white matter: MR evaluation. *AJR Am J Roentgenol* 1987;149:165–71
- Constine LS, Konski A, Ekholm S, et al. Adverse effects of brain irradiation correlated with MR and CT imaging. *Int J Radiation Oncol Biol Phys* 1988;15:319–30
- Wilson DA, Nitschke R, Bowman ME, et al. Transient white matter changes on MRI images in children undergoing chemotherapy for acute lymphocytic leukemia: correlation with neuropsychologic deficiencies. *Radiology* 1991;180:205–09
- Dong Q, Welsh RC, Chenevert TL, et al. Clinical application of diffusion tensor imaging. *J Magn Reson Imaging* 2004;19:6–18
- Khong P-L, Kwong DLW, Chan GCF, et al. Diffusion-tensor imaging for the detection and quantification of treatment-induced white matter injury in children with medulloblastoma: a pilot study. *AJNR Am J Neuroradiol* 2003;24:734–40
- Khong P-L, Leung LHT, Chan GCF, et al. White matter anisotropy in childhood medulloblastoma survivors: association with neurotoxicity risk factors. *Radiology* 2005;236:647–52
- Mabott DJ, Noseworthy MD, Bouffet E, et al. Diffusion tensor imaging of white matter after cranial radiation in children for medulloblastoma: correlation with IQ. *Neuro-Oncol* 2006;8:244–52
- Taylor WD, Mac Fall JR, Provenzale JM, et al. Serial MR imaging of volumes of hyperintense white matter lesions in elderly patients: correlation with vascular risk factors. *AJR Am J Roentgenol* 2003;181:571–76
- Manolio TA, Kronmal RA, Burke GL. Magnetic resonance abnormalities and cardiovascular disease in older adults: the Cardiovascular Health Study. *Stroke* 1994;25:318–27

14. Laskin JJ, Sandler AB. **The role of prophylactic cranial radiation in the treatment of non-small-cell lung cancer.** *Clin Adv Hematol Oncol* 2003;1:731–40
15. Bassar PJ. **Inferring microstructural features and the physiological state of tissues from diffusion-weighted images.** *NMR Biomed* 1995;8:333–44
16. Bassar PJ, Jones DK. **Diffusion tensor MRI: theory, experimental design and data analysis—a technical review.** *NMR Biomed* 2002;14:456–67
17. Kitahara S, Nakasu S, Murata K, et al. **Evaluation of treatment-induced cerebral white matter injury by using diffusion-tensor MR imaging: initial experience.** *AJNR Am J Neuroradiol* 2005;26:2200–06
18. Kim YH, Choi BI, Cho WH, et al. **Dynamic contrast-enhanced MR imaging of VX2 carcinomas after X-irradiation in rabbits: comparison of gadopentetate dimeglumine and a macromolecular contrast agent.** *Invest Radiol* 2003;38:539–49
19. Krueck WG, Schmiedl UP, Maravilla KR, et al. **MR assessment of radiation-induced blood-brain barrier permeability changes in rat glioma model.** *AJNR Am J Neuroradiol* 1994;15:625–32
20. Miot-Noirault E, Akoka S, Hoffschir D, et al. **Potential of T2 relaxation time measurements for early detection of radiation injury to the brain: experimental study in pigs.** *AJNR Am J Neuroradiol* 1996;17:907–12
21. Qiu D, Leung LHT, Kwong PL, et al. **Mapping radiation dose distribution on the fractional anisotropy map: applications in the assessment of treatment-induced white matter injury.** *NeuroImage* 2006;31:109–15
22. Pierpaoli C, Barnett A, Pajevic S, et al. **Water diffusion changes in Wallerian degeneration and their dependence on white matter architecture.** *NeuroImage* 2001;13:1174–85
23. Hein PA, Eskey CJ, Dunn JF, et al. **Diffusion-weighted imaging in the follow-up of treated high-grade gliomas: tumor recurrence versus radiation injury.** *AJNR Am J Neuroradiol* 2004;25:201–09
24. Guo AC, Mac Fall JR, Provenzale JM. **Multiple sclerosis: diffusion tensor MR imaging for evaluation of normal-appearing white matter.** *Radiology* 2002;222:729–36
25. Kaminaga T, Shirai K. **Radiation-induced brain metabolic changes in the acute and early delayed phase detected with quantitative proton magnetic resonance spectroscopy.** *J Comput Assist Tomogr* 2005;29:293–97
26. Maire JP, Coudin B, Guerin J, et al. **Neuropsychologic impairment in adults with brain tumors.** *Am J Clin Oncol* 1987;10:156–62
27. Wassenberg MW, Bromberg JE, Witkamp TD, et al. **White matter lesions and encephalopathy in patients treated for primary central nervous system lymphoma.** *Neurooncol* 2001;52:73–80
28. Steinworth S, Welzel G, Fuss M, et al. **Neuropsychological outcome after fractionated stereotactic radiotherapy (FSRT) for base skull meningiomas: a prospective 1-year follow-up.** *Radiother Oncol* 2003;69:177–82